Differential regulation of closely related R2R3-MYB transcription factors controls flavonol accumulation in different parts of the *Arabidopsis thaliana* seedling

Ralf Stracke[1], Hirofumi Ishihara[1,2], Gunnar Huep[1], Aiko Barsch[2,3], Frank Mehrtens[1], Karsten Niehaus[3] and Bernd Weisshaar[1,*]

[1]*Department of Biology, Genome Research, Bielefeld University, D-33594 Bielefeld, Germany,*

[2]*International NRW Graduate School in Bioinformatics and Genome Research, Bielefeld University, D-33594 Bielefeld, Germany, and*

[3]*Department of Biology, Proteomics and Metabolomics, Bielefeld University, D-33594 Bielefeld, Germany*

OnlineOpen: This article is available free online at www.blackwell-synergy.com

Summary

The genes *MYB11*, *MYB12* and *MYB111* share significant structural similarity and form subgroup 7 of the *Arabidopsis thaliana* R2R3-MYB gene family. To determine the regulatory potential of these three transcription factors, we used a combination of genetic, functional genomics and metabolite analysis approaches. MYB11, MYB12 and MYB111 show a high degree of functional similarity and display very similar target gene specificity for several genes of flavonoid biosynthesis, including *CHALCONE SYNTHASE*, *CHALCONE ISOMERASE*, *FLAVANONE 3-HYDROXYLASE* and *FLAVONOL SYNTHASE1*. Seedlings of the triple mutant *myb11 myb12 myb111*, which genetically lack a complete subgroup of *R2R3-MYB* genes, do not form flavonols while the accumulation of anthocyanins is not affected. In developing seedlings, *MYB11*, *MYB12* and *MYB111* act in an additive manner due to their differential spatial activity; *MYB12* controls flavonol biosynthesis mainly in the root, while *MYB111* controls flavonol biosynthesis primarily in cotyledons. We identified and confirmed additional target genes of the R2R3-MYB subgroup 7 factors, including the UDP-glycosyltransferases UGT91A1 and UGT84A1, and we demonstrate that the accumulation of distinct and structurally identified flavonol glycosides in seedlings correlates with the expression domains of the different R2R3-MYB factors. Therefore, we refer to these genes as *PFG1–3* for '*PRODUCTION OF FLAVONOL GLYCOSIDES*'.

Keywords: flavonoid biosynthesis, *R2R3-MYB*, *PRODUCTION OF FLAVONOL GLYCOSIDES*, gene regulation, Arabidopsis.

Introduction

Flavonoids are widely distributed in the plant kingdom, although they are usually not essential for plant growth. They are classified into flavonols, flavones, isoflavones and anthocyanins (among others) according to the structure of and the modifications to the A, B and C rings of the C_{15} scaffold. Although the most visible function of the flavonoids is the formation of red and purple anthocyanin pigments, non-pigmented flavonoid compounds play central roles in plant biology. They serve as signals for pollinators and other organisms, participate in plant hormone signaling, facilitate pollen-tube growth, protect plants from UV-B

radiation and function as phytoalexins and allelopathic compounds (Harborne and Williams, 2000; Mol *et al.*, 1998; Pietta, 2000; Winkel-Shirley, 2001). The colorless flavonols are among the most abundant flavonoids in plants (Böhm *et al.*, 1998), usually in the form of mono-, di- or triglycosides. Flavonols accumulate in their glycosylated form after an inductive light treatment in the vacuoles of epidermal cells or occasionally in epicuticular waxes (Weisshaar and Jenkins, 1998), absorb UV-B light in the 280–320 nm region and are therefore thought to be effective UV filters (Olsson *et al.*, 1998; Ormrod *et al.*, 1995; Solovchenko and

Schmitz-Eiberger, 2003). There is evidence that auxin retention or transport *in vivo* is regulated by the accumulation of flavonoids, including the flavonols quercetin and kaempferol (Brown *et al.*, 2001; Buer and Muday, 2004; Jacobs and Rubery, 1988; Murphy *et al.*, 2000; Peer *et al.*, 2001). Also, flavonols play a role in human nutrition and have pharmaceutical potential (summarized in Harborne and Williams, 2000; Ross and Kasum, 2002).

The fine regulation of flavonoid biosynthesis (Figure 1) is achieved by combinatorial action(s) of transcription factors, expressed in a spatially and temporally controlled manner (reviewed in Koes *et al.*, 2005; Lepiniec *et al.*, 2006). Regulators belonging to different transcription factor families, including WD40, WRKY, BZIP, MADS-box, R2R3-MYB and basic helix-loop-helix (BHLH) factors, are involved in the transcriptional control of flavonoid biosynthesis genes (*FBG*s) (reviewed in Ramsay and Glover, 2005).

In *Arabidopsis thaliana*, some R2R3-MYB transcription factors have been identified that are involved in the regulation of flavonoid biosynthesis. PRODUCTION OF ANTHO-CYANIN PIGMENT1 (PAP1/MYB75) and PAP2/MYB90 are regulators of genes required for the production of anthocyanins, including *PHENYLALANINE AMMONIUM LYASE* (*PAL*), *CHALCONE SYNTHASE* (*CHS*), *dihydroflavonol 4-reductase* (*DFR*) and *GLUTATHIONE-S-TRANSFERASE* (*GST*; see Figure 1 for full enzyme names). Both factors depend on a BHLH partner that might be present constitutively (Borevitz *et al.*, 2000; Zimmermann *et al.*, 2004). The seed-specific R2R3-MYB factor TRANSPARENT TESTA2 (TT2/MYB123) (Nesi *et al.*, 2001) also needs the interaction with a BHLH factor, namely TT8/BHLH42 (Nesi *et al.*, 2000), to activate the target genes *DFR*, *BANYULS* (*BAN*) and the multidrug and toxic compound extrusion (MATE)-type transporter *TT12*.

Recently, the *A. thaliana* R2R3-MYB factor MYB12 was identified as a flavonol-specific regulator of flavonoid biosynthesis (Mehrtens *et al.*, 2005) that activates in parallel *CHS*, *CHALCONE ISOMERASE* (*CHI*), *FLAVANONE 3-HY-DROXYLASE* (*F3H*) and *FLAVONOL SYNTHASE 1* (*FLS1*). These four flavonol biosynthesis genes are co-regulated in *A. thaliana* (Hartmann *et al.*, 2005) and are required for the formation of the basic flavonol aglycon. MYB12, like the homologous *Zea mays* factor P, does not need a BHLH partner for activation and is suggested to bind similar *cis*-element(s) in the promoters of different target genes (Mehrtens *et al.*, 2005).

There is a lot of apparent structural redundancy among the R2R3-MYB factors that is intensively studied. A prominent example represents the three highly sequence-related factors GLABROUS1 (GL1/MYB0), WEREWOLF (WER/MYB66) and MYB23 which build subgroup 15 (SG15) of the R2R3-MYB family (Kranz *et al.*, 1998; Stracke *et al.*, 2001). WER/MYB66 and GL1/MYB0 are functionally equivalent proteins (Lee and Schiefelbein, 2001) that display their different biological functions in root hair and trichome formation, respectively, only because of their different spatial expression patterns (reviewed in Schiefelbein, 2003). Furthermore, MYB23 has functions redundant to or overlapping with GL1/MYB0 in controlling the initiation of trichome development (Kirik *et al.*, 2001). Another recently published example for redundant R2R3-MYB function is the subgroup 14 (SG14), covering the REGULATORS OF AXIL-LARY MERISTEMS proteins RAX1/MYB37, RAX2/MYB38 and RAX3/MYB84 (Muller *et al.*, 2006), homologous to the tomato (*Solanum lycopersicum*) *BLIND* gene (Schmitz *et al.*, 2002) controlling the formation of lateral meristems in different, but overlapping zones along the shoot axis.

We studied functional redundancy and differential spatial expression characteristics of subgroup 7 (SG7) of the R2R3-MYB factors from *A. thaliana* in the seedling. Subgroup 7 includes the factors MYB11, MYB12 and MYB111 which all display amino acid sequence similarity to ZmP. We show that all members of SG7 are flavonol-specific transcriptional regulators and demonstrate that the final flavonol accumulation pattern is the result of the additive expression patterns of these three factors. Our results indicate that the detailed composition of the flavonols that accumulate in different parts of the *A. thaliana* seedling depends on the differential (tissue- or cell-type-specific) responsiveness of genes that encode flavonol glycosidases, and other enzymes of the downstream part of the biogenesis, to SG7 R2R3-MYB factors.

Results

Identification of potential target genes by transfection experiments

To test whether the two MYB factors MYB11 and MYB111 are functional flavonol-specific transcriptional regulators, their activation potential was tested in co-transfection experiments using *A. thaliana* protoplasts. Potential target gene promoters were fused to the *uidA* ORF (GUS), and standardized β-glucuronidase activity (GUS′) was taken as a measure for target promoter activity. We assayed six promoters for their responsiveness to MYB11 and MYB111 and included MYB12 as an effector control (Figure 2). The *CHS*, *CHI*, *F3H* and *FLS1* gene promoters were responsive to all three assayed R2R3-MYB transcription factors. MYB11 and MYB111 show the highest transactivation capacity for *CHS* with a 36- and 399-fold induction, respectively. Generally, MYB111 displayed stronger transactivation than MYB11. Neither the *flavonoid 3′-hydroxylase* (*F3′H*) nor the *DFR* gene promoters were significantly responsive to MYB11, MYB12 or MYB111 in this assay system. These results show that MYB11, MYB111 and MYB12 have the potential to activate the four flavonol biosynthesis genes required for the formation of the flavonol aglycon.
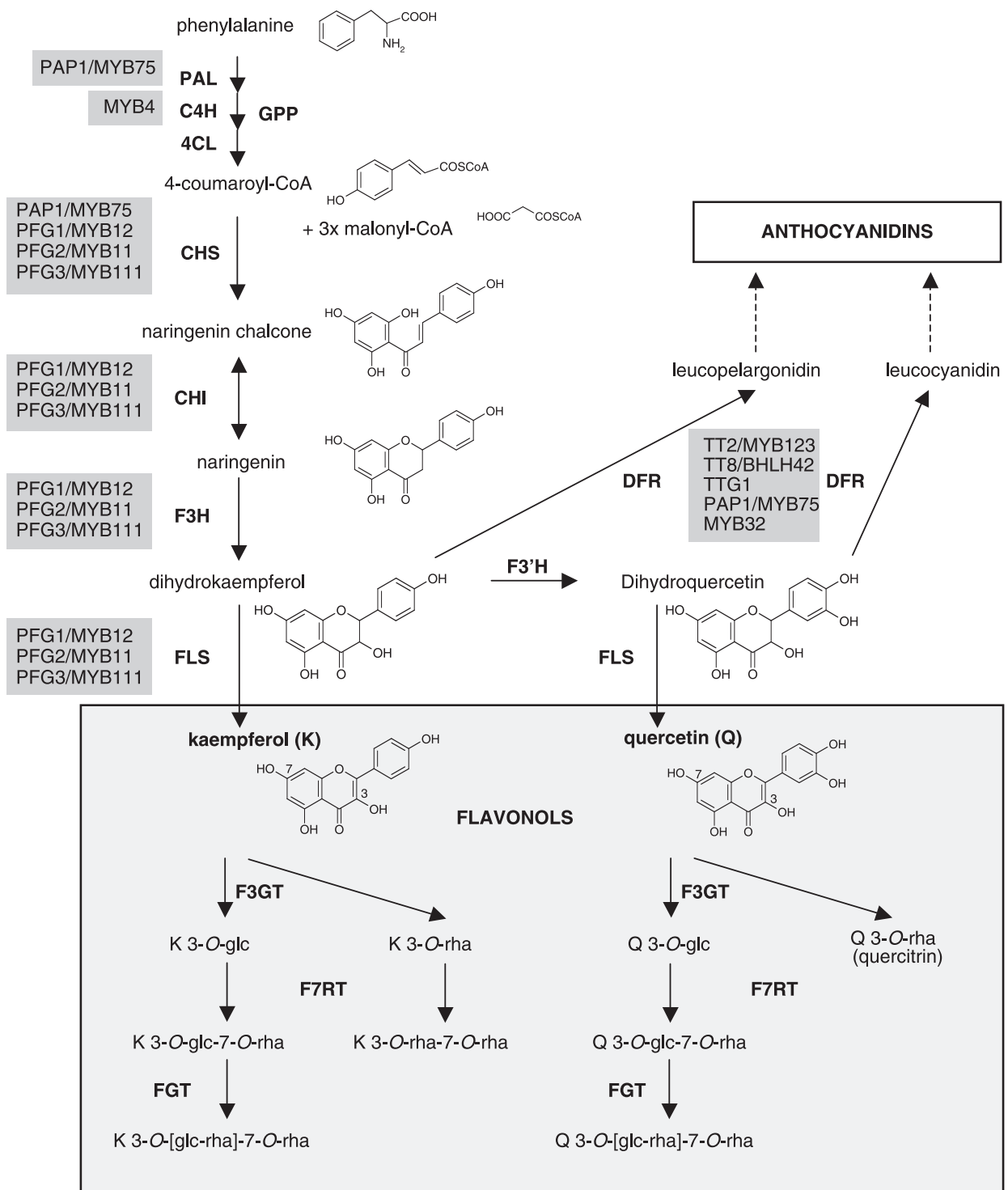
Figure 1. Simplified, schematic representation of the biosynthesis of flavonols and anthocyanins in the *A. thaliana* Col-0 seedling.
To make this figure more comprehensive, the results from this paper have been included. Enzymes are indicated by bold, capital letters. Regulatory proteins are given in gray boxes beside their target genes. Abbreviations are as follows: GPP, general phenylpropanoid pathway; PAL, phenylalanine ammonium lyase; C4H, cinnamate-4-hydroxylase; 4CL, 4-coumaroyl-CoA synthase; CHS, chalcone synthase; CHI, chalcone isomerase; F3H, flavanone 3-hydroxylase; FLS, flavonol synthase; F3'H, flavonoid 3'-hydroxylase; DFR, dihydroflavonol 4-reductase; F3GT, flavonol 3-*O*-glycosyltransferase; F7RT, flavonol 7-*O*-rhamnosyltransferase; FGT, flavonol glycosyltransferase; K, kaempferol; Q, quercetin; K 3-*O*-[glc-rha]-7-*O*-rha, kaempferol 3-*O*-[(rhamnosyl) glucoside]-7-*O*-rhamnoside; Q 3-*O*-[glc-rha]-7-*O*-rha, quercetin 3-*O*-[(rhamnosyl) glucoside]-7-*O*-rhamnoside; PFG, PRODUCTION OF FLAVONOL GLYCOSIDES. Note that the action of FLS is required for the biosynthesis of flavonols (light gray box) while DFR is necessary for the formation of anthocyanidins. Adapted from Routaboul *et al.* (2006). The pathway leading to the formation of isorhamnetin is not illustrated.

Figure 2. Co-transfection analysis of target gene specificities in At7 protoplasts.

Results from co-transfection experiments in *A. thaliana* protoplasts. Promoter fragments of the *CHS*, *CHI*, *F3H*, *FLS*, *F3'H* and *DFR* genes (reporters) were assayed for their responsiveness to the effectors (a) MYB11 (b) MYB111 and (c) MYB12, respectively. The reporter constructs are as described in Mehrtens *et al.* (2005). The figure shows GUS' activity resulting from the influence of tested effector proteins on different reporters. The values above or beside the error bars indicate fold induction values. The mean value of luciferase activity was 6094 relative luminescence units (RLU) μg protein^{-1} sec^{-1} using MYB11 as effector, 1825 RLU μg protein^{-1} sec^{-1} with MYB111 and 6800 RLU μg protein^{-1} sec^{-1} with MYB12.

Identification and characterization of R2R3-MYB *SG7* gene mutants

To examine whether MYB11 and MYB111 are flavonol-specific regulators *in planta*, we isolated Col-0 plants with mutant alleles of these factors by reverse genetics. A *MYB11* and a *MYB111* mutant line with T-DNA insertions in the second and third exon, respectively, were identified (Figure 3). In addition, a homozygous *myb12* mutant carrying a null allele (*myb12*-1f) was used. The homozygous single-mutants are designated in the following by *myb11*, *myb12* and *myb111*, respectively.

Since the three sequence-related *R2R3-MYB* gene products (Figure 3e) seem to have similar functional activity, we included double mutants and the triple mutant in our analyses. The mutants *myb11 myb12*, *myb11 myb111*, *myb12 myb111* and the triple mutant *myb11 myb12 myb11 myb111* did not show any visible difference in comparison to Col-0 wild-type plants when grown under greenhouse conditions.

Expression analysis of R2R3-MYB *SG7 genes in developing seedlings*

To determine SG7 gene transcript levels in developing *A. thaliana* seedlings, quantitative PCR (qPCR) analyses were performed (Figure 4b). In order to discriminate between the three main zones of flavonol accumulation, wild-type seedlings at 5 days after germination (dag) were dissected into three parts (Figure 4a), namely the cotyledons with a small part of the upper hypocotyl (designated C), the hypocotyl-root transition zone and the upper part of the root (H/TZ), and the lower part of the root including the root tip (R). Additionally, whole seedlings (S) were analyzed. *MYB11* transcripts were detected at low levels in all seedling samples. In contrast, *MYB12* and *MYB111* transcripts displayed differential expression patterns with reciprocal expression in roots and cotyledons: *MYB12* transcript levels were predominantly detected in roots where *MYB111* transcripts were hardly detectable, and *MYB111* transcripts showed higher levels in cotyledons where *MYB12* transcript levels were very low. The expression of the three SG7 genes was further examined by promoter:GUS fusion analysis. Transgenic *A. thaliana* plants expressing GUS under the control of 893-bp *MYB11* (*Pro*$_{MYB11}$:*GUS*), 1467-bp *MYB12* (*Pro*$_{MYB12}$:*GUS*) and 1074-bp *MYB111* promoter fragments (*Pro*$_{MYB111}$:*GUS*), respectively, were studied (Figure 4c). *MYB11* promoter activity was found at the region of the apical meristem, the primary leaves, the apex of cotyledons, at the hypocotyl–root transition, the origin of lateral roots and the root tip as well as the vascular tissue of lateral roots. *MYB12* promoter activity was predominantly detected in the root, in the vascular tissue of the hypocotyl–root transition zone and at low levels at the region of apical meristem and the apex of cotyledons. *MYB111*
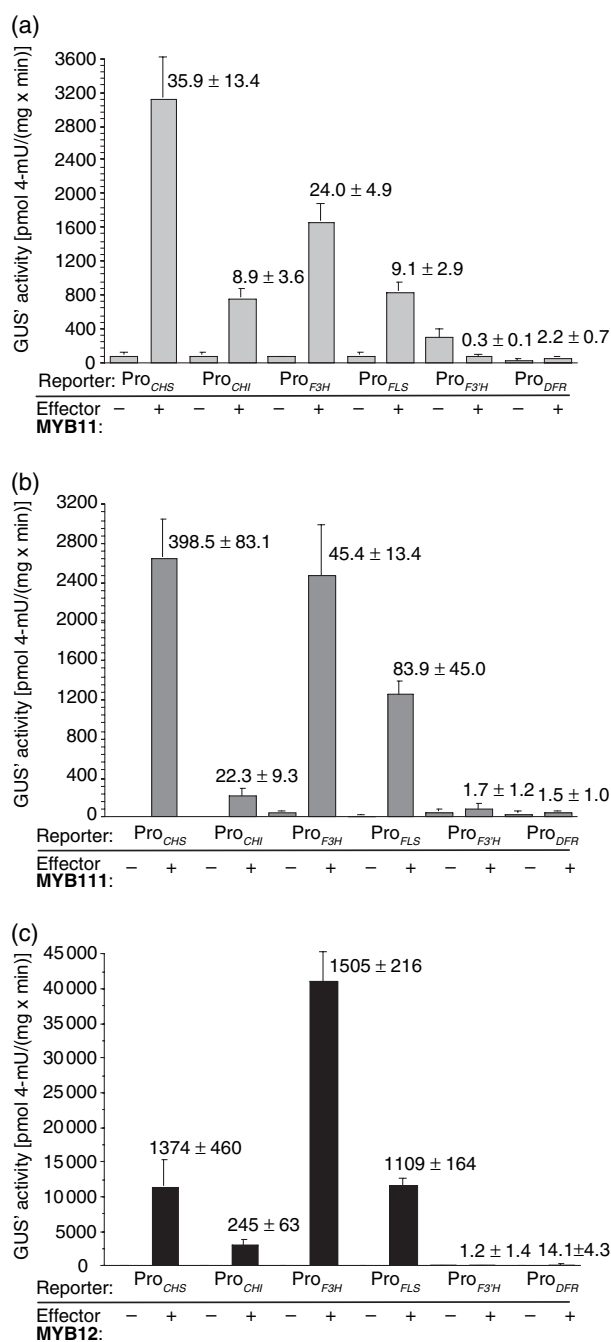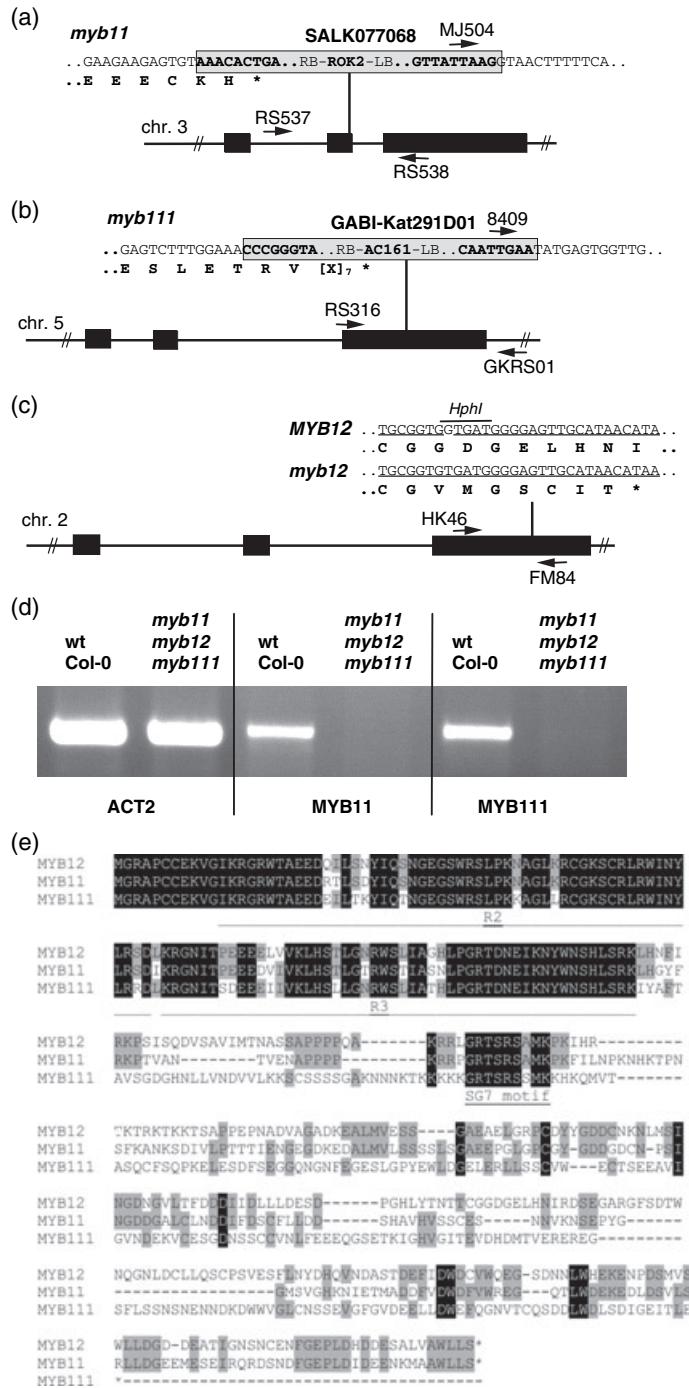
Figure 3. Wild-type and mutant alleles of *R2R3-MYB* SG7 genes.

(a) SALK077068 line with T-DNA insertion in *At3g62610*/*MYB11*. The mutant allele contains a premature Stop codon at codon position 79 of the *MYB11* open reading frame that encodes for 343 amino acids in the wild type.

(b) GABI-Kat291D01 line with a T-DNA insertion in the third exon of *At5g49330*/*MYB111* at amino acid position 204 of 342.

(c) *myb12*-1f knock-out line (Mehrtens *et al.*, 2005). In each panel of (a)–(c) the exon/intron structure is depicted, where black boxes indicate coding regions and thin black lines symbolize non-coding regions. Positions of T-DNA insertions are given as vertical black lines; primers used in PCR genotyping are indicated by arrows and named. See Experimental procedures for primer sequences.

(d) Results from RT-PCR showing the expression of *ACT2*, *MYB11* and *MYB111* in 5-dag *A. thaliana* wild type and SG7 triple mutant seedlings, indicating that *myb11* and *myb111* are null alleles.

(e) Multiple alignment of SG7 R2R3-MYB proteins. Amino acids identical in all three proteins are marked black, amino acids found in two proteins are marked in gray. The R2 and R3 MYB domains as the SG7 motif are marked according to Stracke *et al.* (2001).
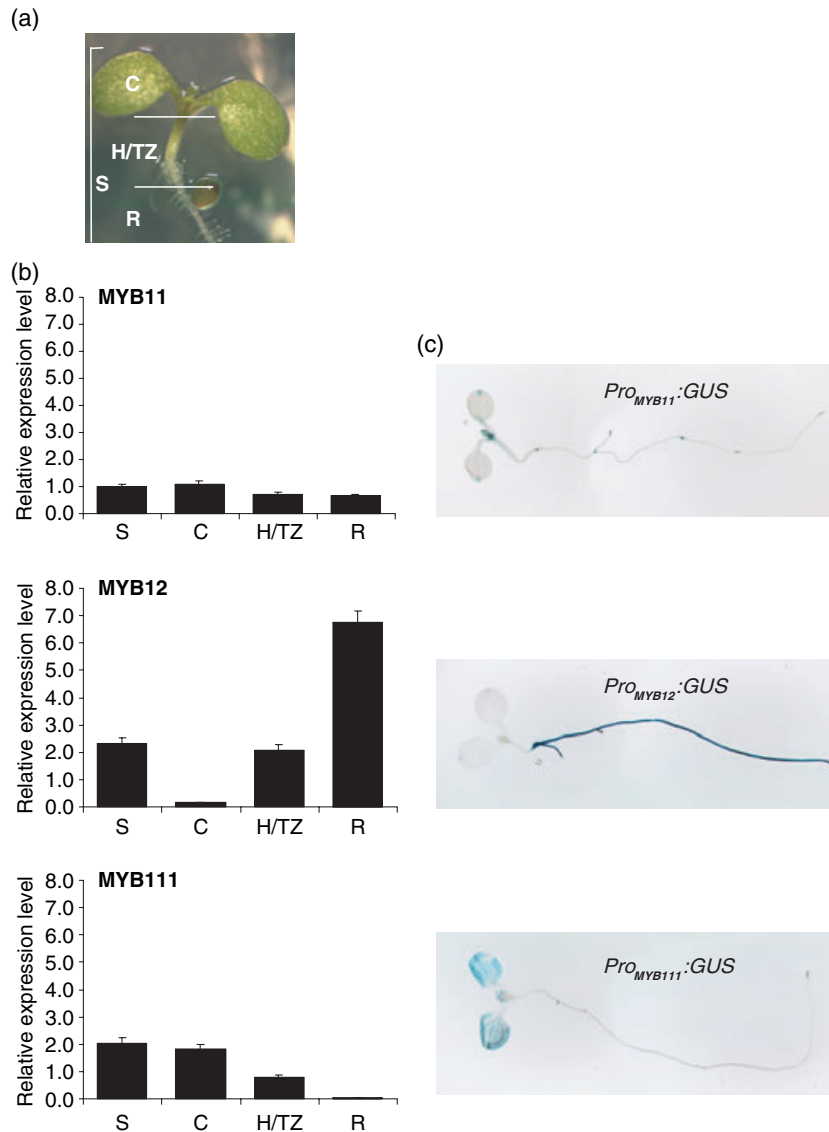
(a)

(b)

(c)

Figure 4. *MYB11*, *MYB12* and *MYB111* are differentially expressed in distinct parts of 5-dag *A. thaliana* Col-0 wild type seedlings.

(a) *Arabidopsis thaliana* seedlings were grown on vertically oriented MS-agar plates and cut into three parts as indicated by the white lines. These three parts represent the different regions of main flavonol accumulation and are referred to as C (cotyledons), H/TZ (hypocotyl/transition zone) and R (root). The whole, uncut seedling is referred to as S.

(b) Quantitative PCR results showing relative expression levels referred to the *MYB11* transcript level in whole seedlings (set as one). Complementary DNA concentrations were normalized to the 18S rRNA transcript levels as standard. Expression was determined in triplicate measurements in two independent biological replicates.

(c) Representative whole mount GUS stainings of Pro$_{MYB11}$:GUS, Pro$_{MYB12}$:GUS and Pro$_{MYB111}$:GUS transformants.

promoter activity was restricted to the cotyledons and primary leaves. Taken together, these data indicate that the *R2R3-MYB* SG7 member *MYB12* is mainly expressed in the root, while *MYB111* is mainly expressed in cotyledons. *MYB11* seems to be expressed at well-defined domains distributed around the developing seedling. These results were obtained with several independent promoter:GUS lines for each promoter, indicating that the observed staining pattern is not due to position effects of the insertion of the transgene.

Screening for SG7 factors' target genes

To screen for additional SG7 MYB target genes we used Affymetrix ATH1 GeneChips (http://www.affymetrix.com/), looking for genome-wide changes in transcript levels caused by the absence of *R2R3-MYB* SG7 gene activity. Hybridizations were conducted with cDNA samples derived from roots of 5-dag Col-0 wild-type seedlings and *myb11 myb12 myb111* seedlings. Since the predominant *R2R3-MYB* SG7 gene expressed in roots is *MYB12*,

Table 1 Screening for SG7 MYB candidate target genes by transcriptome analysis. Expression data obtained from ATH1 GeneChip hybridizations with RNA from roots of 5-dag Col-0 wild type and *myb11 myb12 myb111* triple mutant seedlings. Only genes showing a ≥ 2.5-fold reduction in the mutant and an absolute expression values of ≥ 20 in wild type roots were considered. The identified genes are referred to as candidates since the experiment was designed as a screening transcriptome approach that is not sufficient for detailed statistical analyses value: absolute signal intensity, P: signal is present, A: signal is absent

ATH1 code	AGI code	Wild-type root value		Triple mutant root value		'Fold change'	Name, annotation
247463_at	At5g62210	374.1	P	1.9	A	196.9	Embryo-specific protein 3-related; membrane anchored
251182_at	At3g62600	1026.3	P	22.9	P	44.8	DNAJ heat shock family protein
250207_at	At5g13930	4251.2	P	137.7	P	30.9	CHS; chalcone synthase (TT4)
246467_at	At5g17040	33.9	P	1.6	A	21.2	UDP-glucoronosyl/UDP-glucosyl transferase family protein
265290_at	At2g22590	96.4	P	6.0	A	16.1	Glycosyltransferase family protein (UGT91A1)
250533_at	At5g08640	1176.9	P	75.9	P	15.5	FLS1; flavonol synthase
251827_at	At3g55120	895.7	P	63.7	P	14.1	CHI; chalcone isomerase (TT5)
248625_at	At5g48880	656.7	P	65.7	P	10.0	Acetyl-CoA C-acyltransferase 1 / 3-ketoacyl-CoA thiolase 1 (PKT1)
261907_at	At1g65060	299.1	P	36.8	P	8.1	4CL3; 4-coumarate:CoA ligase 3
245560_at	At4g15480	220.8	P	29.2	A	7.6	UDP-glucoronosyl/UDP-glucosyl transferase family protein (UGT84A1)
250467_at	At5g10100	21.7	P	3.3	A	6.6	Trehalose-6-phosphate phosphatase
250558_at	At5g07990	327.8	P	51.2	P	6.4	F3'H; flavonoid 3'-monooxygenase/flavonoid 3'-hydroxylase (TT7)
251191_at	At3g62590	28.6	P	6.4	A	4.5	Lipase class 3 family protein
245567_at	At4g14630	26.2	P	5.9	A	4.4	Germin-like protein (GLP9)
250794_at	At5g05270	586.9	P	132.7	P	4.4	Chalcone-flavanone isomerase family protein
266578_at	At2g23910	409.6	P	102.9	P	4.0	Cinnamoyl-CoA reductase-related protein
250620_at	At5g07190	50.9	P	13.3	A	3.8	Embryo-specific protein 3
265422_at	At2g20800	32.7	P	9.8	A	3.3	Pyridine nucleotide-disulphide oxidoreductase family protein
256940_at	At3g30720	26.7	P	8.2	P	3.3	Expressed protein
266900_at	At2g34610	73.3	P	23.4	P	3.1	Expressed protein
263268_at	At1g33860	30.1	P	9.7	A	3.1	Hypothetical protein
253669_at	At4g30000	37.1	P	12.6	P	2.9	Dihydropterin pyrophosphokinase, putative dihydropteroate synthase
248564_at	At5g49700	24.1	P	8.3	A	2.9	DNA-binding protein-related
252123_at	At3g51240	2102	P	728	P	2.9	F3H; flavanone 3-hydroxylase (TT6)
253195_at	At4g35420	94.7	P	32.9	P	2.9	Dihydroflavonol 4-reductase family protein
252215_at	At5g34930	21.3	P	7.7	P	2.8	Arogenate dehydrogenase
266851_at	At2g26820	24.3	P	8.8	A	2.8	Avirulence-responsive family protein
261773_at	At1g76250	28.5	P	10.4	A	2.7	Expressed protein
258241_at	At3g27650	52.9	P	19.4	A	2.7	Lateral organ boundaries (LOB) domain protein 25 (LBD25)
266618_at	At2g35480	27.4	P	10.2	A	2.7	Expressed protein
259136_at	At3g05470	20.6	P	7.7	P	2.7	Formin homology 2 domain-containing protein
244934_at	Atcg01080	57.3	P	21.5	A	2.7	NADH dehydrogenase ND6 (chloroplast encoded, Atc)
252128_at	At3g50870	20.3	P	7.7	P	2.6	Zinc finger (GATA type) family protein, GATA transcription factor 3
260558_at	At2g43600	37.6	P	14.4	P	2.6	Glycoside hydrolase family 19 protein
253638_at	At4g30470	340.2	P	132	P	2.6	Cinnamoyl-CoA reductase-related protein
247020_at	At5g67020	22.1	P	8.6	A	2.6	Expressed protein
260643_at	At1g53270	42.6	P	17	P	2.5	ABC transporter family protein
256376_s_at	At1g66690	25.2	P	10.1	P	2.5	*S*-adenosyl-L-methionine:carboxyl methyltransferase family protein
261496_at	At1g28360	26.4	P	10.7	P	2.5	ERF domain protein 12 (ERF12)

Value is the absolute signal intensity; P, signal is present; A, signal is absent.

this experimental design mainly addresses genes regulated by *MYB12* and avoids at least in part complications caused by the activation of other phenylpropanoid biosynthesis genes in the aerial part of the seedling. When evaluating expression levels for reduction in the triple mutant compared to wild type, a number of 'downregulated genes' were identified (see Table 1). These include genes encoding known flavonoid biosynthetic enzymes (*CHS*, *At5g13930*; *FLS1*, *At5g08640*; *CHI*, *At3g55120*; *F3'H*, *At5g07990*; *F3H*, *At3g51240*) and one encodes one of four 4-coumarate-CoA ligase isoenzymes (*4CL3*, *At1g65060*) which act in the general phenylpropanoid pathway (see Figure 1). In addition to genes encoding enzymes of flavonol aglycon biosynthesis and a number of unknown genes, several genes annotated to encode glycosyltransferases (*At5g17040*, *At2g22590* and *At4g15480*) were among the candidates for being responsive to R2R3-MYBs of SG7. Since flavonols accumulate in their glycosylated form, the detection of these glycosyltransferase genes fits well to the expectations for transcriptional control of the production of specific flavonol derivatives.

Confirmation of candidate target genes

We used qPCR and co-transfection assays to verify the results of the transcriptome analysis screening and to check whether SG7 R2R3-MYB factors are able to directly activate the promoters of three candidate genes identified. The most responsive gene *At5g62210* which encodes a membrane anchored protein of unknown function and two genes coding for the glycosyltransferases UGT91A1 (*At2g22590*) and UGT84A1 (*At4g15480*) which displayed the highest absolute signal values among all UGTs in the wild-type sample were chosen. All three putative target genes displayed strongly reduced transcript levels in the triple mutant (Figure 5a), verifying the results obtained from the ATH1 chip hybridizations. We also tested the responsiveness of the gene promoters (Pro$_{At5g62210}$, Pro$_{At2g22590}$ and Pro$_{At4g15480}$) to SG7

factors in co-transfection experiments using At7 protoplasts (Figure 5b). All three candidate promoters were highly responsive to MYB12, MYB111 and MYB11. In conclusion, the results from the screening are validated by qPCR data and the transient *in vivo* assay. As already observed for the promoters of the genes required for flavonol aglycon biosynthesis, the activating potential decreases from MYB12 via MYB111 to MYB11.

Flavonol accumulation analysis of mutant seedlings and identification of flavonol derivatives

To be able to correlate gene expression data with the accumulation of flavonols in different parts of the seedling, we analyzed the secondary metabolite constituents of the single, double and triple mutant seedlings by high-perform-
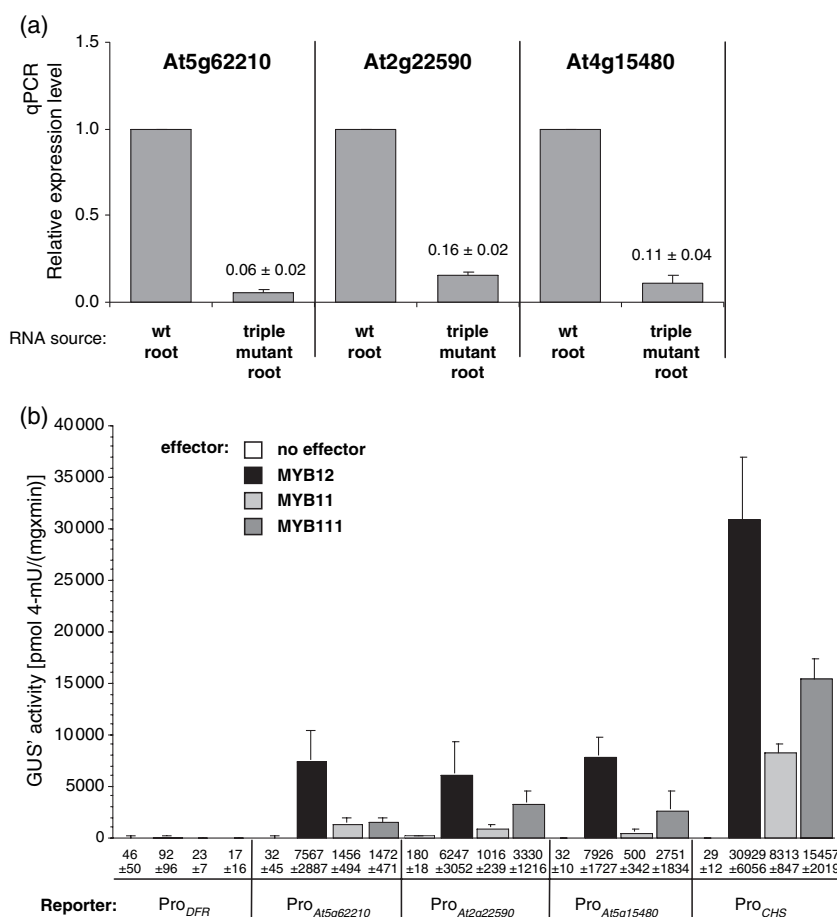

Figure 5. Confirmation of candidate SG7 R2R3-MYB target genes.
(a) Confirmation of microarray results. Results from qPCR showing the relative expression of *At5g62210*, *At2g22590* and *At4g15480* in roots of *A. thaliana* Col-0 wild type and *myb11 myb12 myb111* triple mutant 5-dag seedlings. Columns represent the relative expression levels of distinct target genes tested. Values were normalized to 18S rRNA and relative expression levels were referenced to the amount of mRNA in the wild-type sample. The values above the bars indicate the fold increase in the mutant.
(b) Co-transfection analysis of activation potential in At7 protoplasts. Results from co-transfection experiments in *A. thaliana* protoplasts. Promoter fragments of *At5g62210*, *At2g22590*, *At4g15480* and *DFR*, *CHS* (as controls) were tested on their responsiveness to MYB11, MYB12 and MYB111 as effector. The figure shows absolute GUS' activity resulting from the influence of MYB protein on the different reporters. The mean value of luciferase activity was 2516 RLU μg protein^{-1} sec^{-1} for MYB11, 3366 RLU μg protein^{-1} sec^{-1} for MYB12 and 2350 RLU μg protein^{-1} sec^{-1} for MYB111.
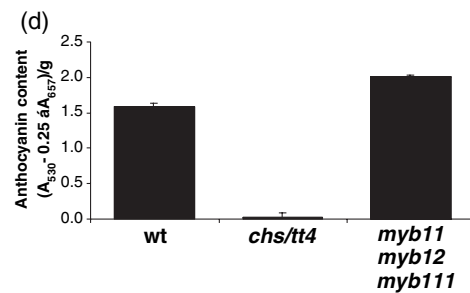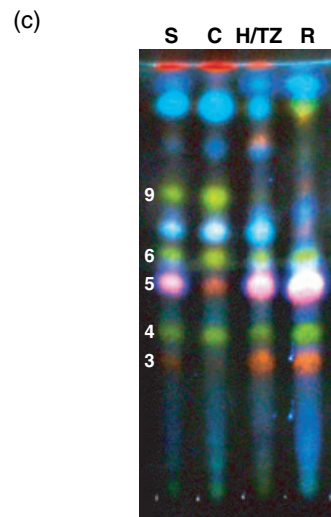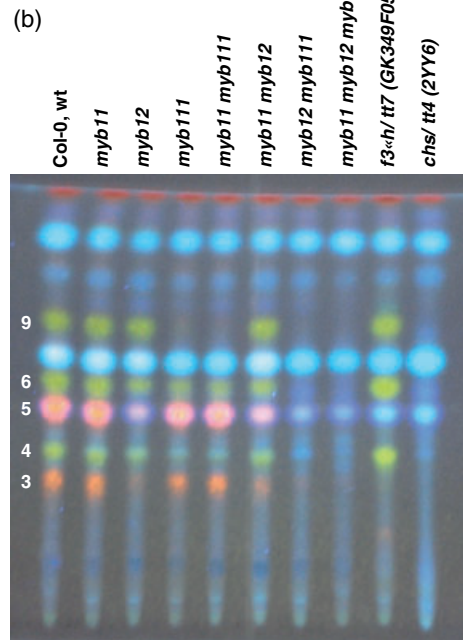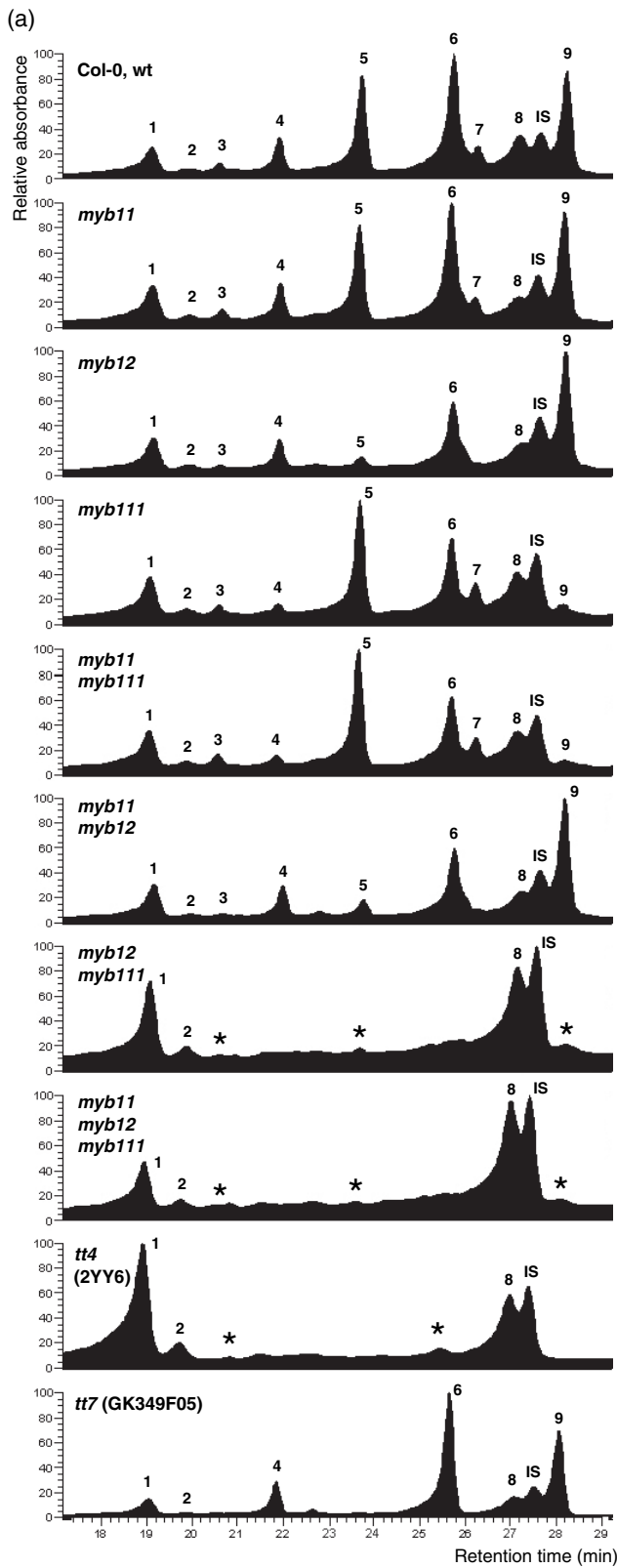
Table 2 Identification of flavonol derivatives in methanolic extracts of Col-0 seedlings. Structure identification of flavonol derivatives extracted from HPTLC plates was performed using a successive combination of HPLC-PDA-ESI/MS. Sugar analysis of flavonol glycosides was performed with GC/MS. Flavonol derivatives were identified by comparison with MS results and known flavonol glycosides from the literature (Graham et al., 1998; Jones et al., 2003; Routaboul et al., 2006; Stobiecki et al., 2006; Tohge et al., 2005). RT: retention time, ESI/MS: ElectroSpray Ionization/ Mass Spectrometry, m/z: mass/charge ratio, MSn: tandem mass spectrometry, qr: quercetin, km: kaempferol, glc: glucose, rha: rhamnose, n.a.: not analyzed, IS: internal standard. [a]Detected in MS and/or in tandem mass spectrometry (MSn) data

Peak	RT (min)	ESI/MS (m/z)	Fragment[a] (m/z)	Compound name
1	18.85	387 $[M + H]^+$	n.a.	Sinapate glucoside
		409 $[M + Na]^+$		
2	19.70	773 $[2M + H]^+$	n.a.	Sinapate derivative
		795 $[2M + Na]^+$		
3	20.40	757 $[M + H]^+$	303 $[qr + H]^+$	Quercetin [rhamnosyl-glucoside]-rhamnoside
		779 $[M + Na]^+$	449 $[qr + rha + H]^+$	
			611 $[qr + rha + glc + H]^+$	
4	21.75	741 $[M + H]^+$	287 $[km + H]^+$	Kaempferol [rhamnosyl-glucoside]-rhamnoside
		763 $[M + Na]^+$	433 $[km + rha + H]^+$	
			595 $[km + rha + glc + H]^+$	
5	23.50	611 $[M + H]^+$	303 $[qr + H]^+$	Quercetin glucoside-rhamnoside
		633 $[M + Na]^+$	449 $[qr + rha + H]^+$	
6	25.45	595 $[M + H]^+$	287 $[km + H]^+$	Kaempferol glucoside-rhamnoside
		617 $[M + Na]^+$	433 $[km + rha + H]^+$	
7	25.95	625 $[M + H]^+$	339 $[IR + Na]^+$	Isorhamnetin glucoside-rhamnoside
		647 $[M + Na]^+$	501 $[IR + glc + Na]^+$	
8	26.90	681 $[M + H]^+$	n.a.	Sinapate derivative
		703 $[M + Na]^+$		
9	27.95	579 $[M + H]^+$	287 $[km + H]^+$	Kaempferol rhamnoside-rhamnoside
		601 $[M + Na]^+$	433 $[km + rha + H]^+$	
IS	27.30	449 $[M + H]^+$	n.a.	Luteolin 7-glycoside (internal standard)

RT, retention time; ESI/MS, electrospray ionization/mass spectrometry; m/z, mass/charge ratio; qr, quercetin; km, kaempferol; glc, glucose; rha, rhamnose; n.a., not analyzed; IS, internal standard.
[a]Detected in MS and/or in tandem mass spectrometry data.

ance liquid chromatography (HPLC). Phenylpropanoid compounds were extracted from the SG7 *myb* mutants, from Col-0 wild type, and from two *transparent testa* (*tt*) mutants with Col-0 genetic background. *chs/tt4*-2YY6, a mutant that lacks flavonoids, and *f3'h/tt7*-GK349F05, a mutant lacking quercetins (see Figure 1).

Clearly detectable HPLC peaks in the wild-type sample were numbered from 1 to 9 with increasing retention times as shown in Figure 6(a). In addition, the extracts were analyzed by high-performance thin layer chromatography (HPTLC; Figure 6b). The fluorescence color of the diphenylboric acid 2-aminoethylester (DPBA)-stained

phenylpropanoids provides information about their basic chemical structure. In the Col-0 sample, three kaempferol derivatives (green), two quercetin derivatives (orange) and up to seven sinapate derivatives (blue) were detectable.

Flavonol derivatives detected by HPLC and HPTLC were correlated with each other by HPLC analysis of HPTLC-separated compounds that had been re-extracted from the plates. The results are summarized in Figure 6(b) by numbering the spots on the HPTLC plate with the peak numbers from HPLC. Subsequently, the chemical nature of the respective compounds was analyzed by a successive com-

Figure 6. Metabolic analyses of methanolic extracts of mutant seedlings.
(a) Typical representative HPLC-PDA chromatograms (monitored by absorbance at 354 nm) obtained from 80% methanolic extracts of 5-dag *A. thaliana* seedlings of the indicated genotypes. Peaks are numbered in the chromatogram of Col-0 wild-type seedlings, where IS is the abbreviation for the internal standard used for quantification, the digitoflavone luteolin-7-glycoside. Peaks were classified by UV spectral analysis as corresponding to flavonol or sinapate derivatives. Minor peaks with UV spectra that do not fit to the known spectrum of flavonols are indicated by asterisks.
(b) Representative result of the same methanolic extracts analyzed in (a) after separation by HPTLC on silica gel-60 plates followed by DPBA staining. Pictures were taken under UV illumination. Color key: green, kaempferol derivative; orange, quercetin derivative; faint blue, sinapate derivative; pink, overlapping quercetin and sinapate derivatives; dark red, chlorophyll. Numbers given at the left correspond to the peak numbers as mentioned in (a). Names of identified structures are indicated in Table 2.
(c) The HPTLC analysis of methanolic extracts showing different flavonoid compositions in distinct parts of 5-dag *A. thaliana* Col-0 wild-type seedlings. Peak numbers are as in (a) and (b). *Arabidopsis thaliana* seedlings were grown and cut as described in the legend of Figure 4: C, cotyledons; H/TZ, hypocotyl/transition zone; R, root; S, whole uncut seedling.
(d) Photometric determination of the anthocyanin content in acidic methanolic extracts of *A. thaliana* seedlings: A_{530}, absorption at 530 nm; A_{657}, absorption at 657 nm.

bination of HPLC–photodiode array (PDA) analyses and electrospray ionization/mass spectroscopy (ESI/MS). Sugar analyses of flavonol glycosides were achieved by gas chromatography-mass spectroscopy (GC-MS). The results including the ESI/MS mass/charge ratios are summarized in Table 2. Finally, the combination of the various chromatographic and spectroscopic methods, and comparison with published data (see legend of Table 2) allowed the identification of two quercetin derivatives (peak 3, quercetin 3-*O*-[(rhamnosyl) glucoside]-7-*O*-rhamnoside; peak 5, quercetin 3-*O*-glucoside-7-*O*-rhamnoside) and three kaempferol derivatives (peak 4, kaempferol 3-*O*-[(rhamnosyl) glucoside]-7-*O*-rhamnoside; peak 6, kaempferol 3-*O*-glucoside-7-*O*-rhamnoside; peak 9, kaempferol 3-*O*-rhamnoside-7-*O*-rhamnoside). This identification also fits the expected compound accumulation patterns for the *tt* mutants analyzed, that are the lack of flavonols in *chs/tt4*-2YY6 and the lack of quercetins in *f3′h/tt7*-GK349F05.

The data show a selective reduction of specific flavonol derivatives in the different mutants, indicating that MYB12 and MYB111 direct the accumulation of flavonol derivatives that differ with respect to hydroxylation and glycosylation patterns.

HPTLC profiling of different parts of the wild-type seedling

To investigate whether the expression domains of the SG7 *MYB* genes display differential secondary metabolite accumulation patterns, we analyzed extracts from the three parts of wild-type seedlings described above (C, H/TZ, R,S; see Figure 4a) by HPTLC/DPBA staining. Clear differences in the pattern of accumulation of phenylpropanoid compound in the different parts of the seedlings were observed (Figure 6c). The kaempferol–rhamnoside–rhamnoside band (peak 9) is absent in the root, while the quercetin–[(rhamnosyl) glucoside]–rhamnoside band (peak 3) is drastically reduced in the cotyledons. In the hypocotyl–root transition zone and the root additional compounds become detectable. These compounds seem to be under-represented in the seedling (S) sample due to dilution effects and were therefore not covered by the compound characterization described above.

The metabolic profiles detected for the seedling parts are in accordance with the accumulation data obtained from mutant seedlings and the expression patterns of the different SG7 factors. For example, MYB111 expressed in cotyledons controls the accumulation of kaempferol–rhamnoside–rhamnoside (peak 9); peak 9 is found in cotyledons but not in other parts of the seedlings, and is missing in the *myb111* mutant.

In summary, the accumulation data indicate that there is organ specificity with regard to accumulation of phenylpropanoid in the seedling that is to a large extend controlled by SG7 R2R3-MYB factors.

Analysis of anthocyanin content

Based on the information about the biochemical pathway (see Figure 1), we reasoned that changes in the activity of SG7 factor may affect the formation of anthocyanins in the seedling because *CHS* is a target gene of the SG7 factors and is required for anthocyanidin biosynthesis. Anthocyanins are present in the Col-0 wild-type seedling but are absent from the *chs/tt4*-2YY6 mutant (Figure 6d). Anthocyanins were clearly detectable in the *myb11 myb12 myb111* mutant seedlings, demonstrating that CHS and DFR are active in the triple *myb* mutant. The level to which anthocyanins accumulate in the triple *myb* mutant is slightly but reproducibly higher than in the wild type, indicating that precursors usually channeled to flavonols are used to form anthocyanins. We concluded that in the seedling part which is programmed to synthesize anthocyanins the flavonoid biosynthesis genes are under the control of factors different from the R2R3-MYBs of SG7.

In situ *flavonoid staining of mutant seedlings*

The distribution of flavonol accumulation in the various *myb* mutant and wild-type seedlings was visualized with DPBA and imaged by epifluorescence microscopy. Representative pictures are shown in Figure 7. In the wild-type, the cotyledons show intense orange fluorescence indicating a massive accumulation of flavonols. Also the hypocotyl, the hypocotyl–root transition zone, the root vascular tissue and the root tip display orange staining indicative of flavonols. The *chs/tt4*-2YY6 and *f3′h/tt7*-GK349F05 mutants were included as controls and either do not show any staining (absence of flavonols in the *chs/tt4* mutant) or display greenish kaempferol-specific staining (*f3′h/tt7* mutant). The triple mutant *myb11 myb12 myb111* essentially displays staining identical to that of the *chs/tt4*-2YY6 mutant, confirming the absence of flavonols in seedlings that lack *R2R3-MYB* SG7 activity.

Consistent with the data presented above, the *myb11* seedlings did not significantly differ in flavonol accumulation from wild type. On the other hand, the *myb12 myb111* double mutant showed a staining similar to that of the triple mutant with the exception of a faint orange staining at the apical meristem region, the tips of the cotyledons (Figure 7b) and in some cases at the root tip (data not shown). Clearly different spatial flavonol accumulation patterns were obtained for *myb12* and *myb111* seedlings. The *myb12* mutant seedlings display drastically reduced flavonol levels in the root and the hypocotyl–root transition zone, while *myb111* mutant seedlings lack flavonols in the cotyledons. In conclusion, the *in situ* visualization of flavonols in the seedling clearly supports the differential accumulation of flavonols in different parts of the seedling as a function of the expression of different R2R3-MYB SG7 factors.
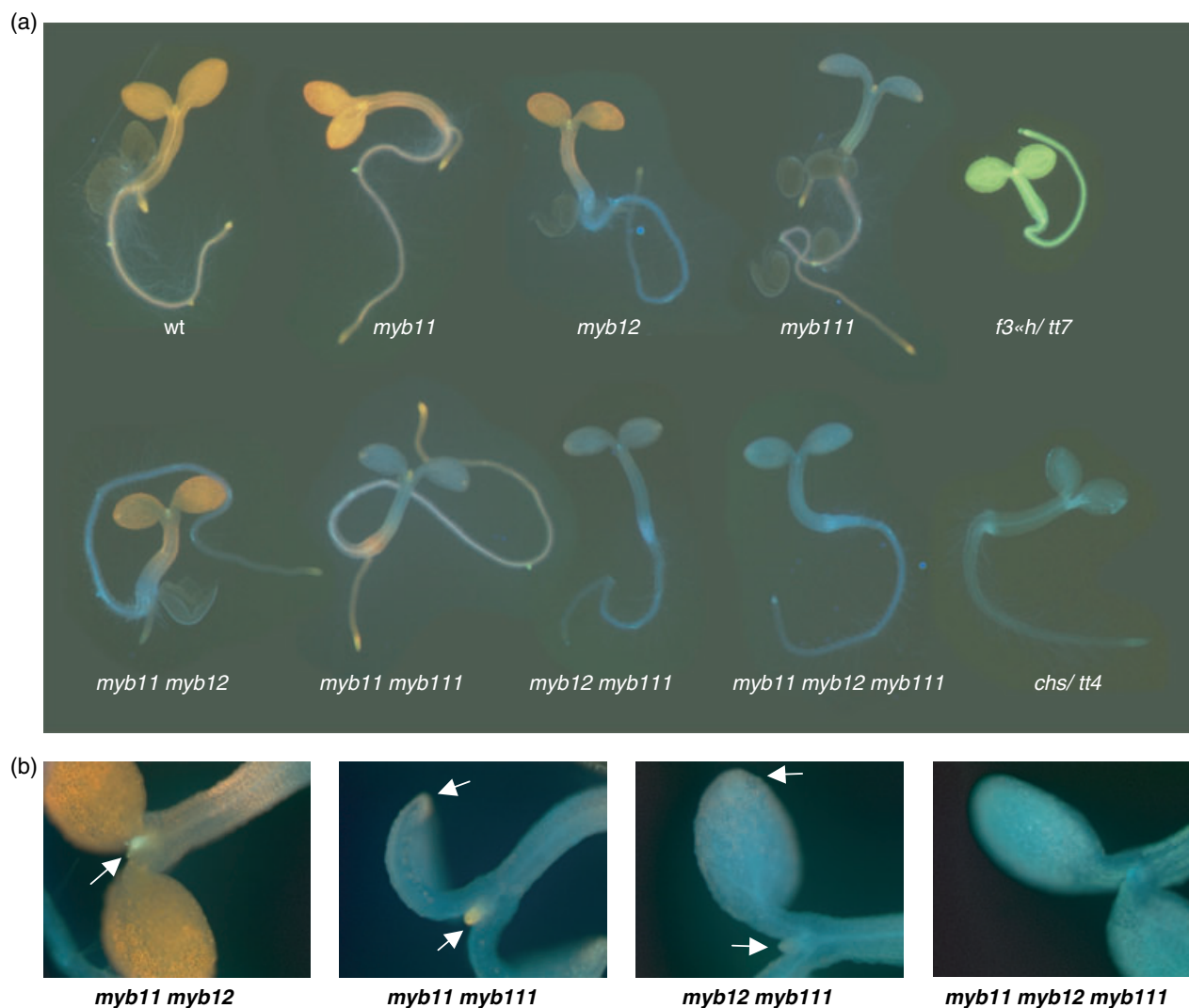
(a)

(b)

myb11 myb12 **myb11 myb111** **myb12 myb111** **myb11 myb12 myb111**

Figure 7. Flavonol staining in wild-type and mutant seedlings.
(a) Flavonols in intact, norflurazon-bleached seedlings were stained with DPBA until saturation and imaged by epifluorescence microscopy. Photographs of representative seedlings are shown.
(b) Close-ups to show accumulations of flavonol at the apical meristem region and at the tip of cotyledons, indicated by arrows. The greenish color at the apical meristem region in the *myb11 myb12* mutant indicates accumulation of kaempferol derivatives, while orange indicates quercetin derivatives in the other double mutants.

Discussion

In wild-type *A. thaliana* seedlings flavonols accumulate in three main zones: the cotyledonary node, the hypocotyl–root transition zone and the root tip (Murphy *et al.*, 2000; Peer *et al.*, 2001; Saslowsky and Winkel-Shirley, 2001; Sheahan and Rechnitz, 1993). The flavonol accumulation pattern we observed by *in situ* DPBA staining in Col-0 wild-type seedlings is in strict accordance with that found for the accumulation of aglycone flavonols in 5-day-old *A. thaliana* seedlings of the Landsberg *erecta* accession (Murphy *et al.*, 2000; Peer *et al.*, 2001). The *chs/tt4* mutant is not able to synthesize flavonoids; consequently no flavonols are detected in

seedlings containing the *chs* null alleles *tt4*-2YY6 (Col-0; Burbulis *et al.*, 1996) or *tt4*-1 (L*er*; Sheahan and Rechnitz, 1992). The observed faint blue coloration in *tt4* seedlings is probably a result of accumulation of sinapate ester (Saslowsky *et al.*, 2000), an interpretation that is confirmed by our HPTLC data. The *myb* triple mutant displayed the same lack of flavonols as a *tt4* null mutant. We concluded that a lack activity of *R2R3-MYB* SG7 genes in seedlings causes the absence of flavonols only, while the accumulation of anthocyanins is essentially not affected. In contrast to the situation in *tt4*, SG7 triple mutant seedlings show anthocyanin accumulation in the seedlings (Figure 6d) and normal pigmentation of the seed produced by adult plants (data not shown). In fact,

the anthocyanin level in SG7 triple mutant seedlings was slightly higher than in the wild type. This observation is consistent with a presumed rechanneling of flavonol precursors to the anthocyanin branch of the pathway which is also known from the *ban* mutation (Albert *et al.*, 1997) that causes anthocyanin accumulation in the seed coat.

The SG7 triple mutant is the first described *A. thaliana* line that produces seedlings which specifically lack flavonols but not other flavonoids. Therefore, the mutant is a useful tool for the analyses of the functions attributed to flavonols, like their influence on light or gravity responses (Buer and Muday, 2004; Buer *et al.*, 2006; Peer *et al.*, 2001) or their capacity to repress bud outgrowth that affects lateral branching (Lazar and Goodman, 2006). In this biological context preliminary experiments showed no measurable altered gravitropic response, nor a distinctive branching pattern in the triple *myb* mutant (data not shown). This lack of phenotypes may indicate that these traits are not due to the lack of flavonols.

The apparent differential spatial accumulation pattern of flavonol obtained in *myb12* and *myb111* seedlings was shown to be a function of differential expression of R2R3-MYB SG7 factors. Clearly, MYB12 and MYB111 are the main regulators of flavonol biosynthesis in seedlings. There exists an obvious 'job sharing' between the *R2R3-MYB* SG7 genes in regulating similar target genes from the main flavonoid pathway required for the formation of the flavonol aglycon in different locations, that is traced back to different expression domains of the individual genes in the *A. thaliana* seedling. On the basis of the results discussed above, we rename the *R2R3-MYB* genes from SG7 as *PRODUCTION OF FLAVONOL GLYCOSIDES1–3*, namely *PFG1/MYB12*, *PFG2/MYB11* and *PFG3/MYB111*.

SG7 R2R3-MYB target genes

Since the single *myb* mutants were shown to affect different flavonol derivatives, it is conceivable that the individual PFG factors also regulate different target genes that are involved in the formation of specific flavonol compounds. From the available results, particularly the metabolite analysis in the *pfg* mutants (Figure 6b), we assume that the synthesis of some specific flavonol glycosylates seems to be mainly controlled by one PFG transcription factor (e.g. synthesis of kaempferol-rhamnoside-rhamnoside, peak 9 by PFG3/ MYB111), while others seem to be regulated by more than one PFG factors (e.g. synthesis of kaempferol–glucoside– rhamnoside, peak 6 by PFG1/MYB12 and PFG3/MYB111). However, it remains to be determined whether differences in the modification pattern in the various seedling organs are due to differences in the set of target genes of individual PFG factors. It is possible that additional organ- or tissue-specific factors positively or negatively regulate the expression of genes acting on the modification processes.

We have assayed the promoters of six different FBGs in co-transfection experiments, but we must assume that the PFG factors also control the activity of additional target genes that are involved in flavonol biosynthesis. On the basis of the biochemical phenotype (chemotype), we hypothesize that all three factors are flavonol-specific regulators and that they do not activate genes encoding enzymes with exclusive specificity for other branches of flavonoid biosynthesis. This hypothesis is supported by biochemical data from the PFG1/MYB12-overexpression line (Mehrtens *et al.*, 2005) and the transcriptome analysis presented in this work. Nevertheless, the regulon of PFG factors is not restricted to the pathway starting with CHS and ending with FLS. The ATH1 chip hybridization results (Table 1) indicated that in addition to the flavonol aglycon biosynthesis genes also the *4CL3* gene is activated. 4-Coumaroyl-CoA synthase 3 (4CL3) catalyses one of the three enzymatic steps of the general phenylpropanoid pathway (GPP, see Figure 1). We conclude that the PFG regulon also covers parts of the genes from the GPP. Such coordinated regulation of GPP genes together with genes belonging to specific branches of the flavonoid biosynthesis pathway also occurs by PAP1/MYB75 (Borevitz *et al.*, 2000; Tohge *et al.*, 2005) which activates the GPP gene *PAL1* and anthocyanin-specific genes, and also for MYB4 (Jin *et al.*, 2000) which represses the GPP gene *C4H* and genes encoding enzymes of hydroxycinnamic acid metabolism.

F3'H was also observed as potential PFG target in the transcriptome analysis, although this gene seems not to be a target in the co-transfection assay (Figure 2). This can be explained: (i) by 'metabolic feedback' that takes place *in planta* (Jorgensen *et al.*, 2005; Winkel-Shirley, 1999) and (ii) by the assumption that for the activation of the *F3'H* in At7 protoplasts an unknown additional co-factor is required that might not be present in the cultured At7 cells, or because the 1291-bp *F3'H* promoter fragment used in co-transfection assays does not cover the full-length promoter.

Other noteworthy putative PFG target genes are *At1g53270*, encoding an ABC transporter family protein, and *At5g34930*, encoding an arogenate dehydrogenase. The ABC transporter might be able to facilitate the transport of flavonols across the tonoplast. In the study of Tohge *et al.* (2005) two transporters encoded by the genes *At1g34580* and *At4g04750*, as well as the MATE-type transporter TT12 (Debeaujon *et al.*, 2001), which has been proposed to load pro-vacuoles with flavonoid intermediates required for proanthocyanin biosynthesis, were identified as putative targets of the anthocyanin-specific regulator PAP1/MYB75. Arogenate dehydrogenases are known to be involved in the biosynthesis of aromatic amino acids (Lingens and Keller, 1983), covering the synthesis of phenylalanine, being the entry substrate of the GPP. It seems that the transcription factor regulons reach from the phenylalanine biosynthesis, GPP genes, the FBGs required for aglycon formation, genes

for modifying functions like glycosidases (see below) down to transporters which are potentially specific for different flavonoid classes. Obviously, this hypothesis has to be proven in the future by analyzing mutants in the respective genes for their chemotype.

Regarding the genes encoding functions that modify the flavonol aglycon, the genes that code for the glycosyltransferases UGT91A1 and UGT84A1 (Bowles, 2002) were confirmed to be targets of all three PFGs (Figure 5). Since the degree and function of glycosylation of flavonols have not yet been characterized in detail, and genetic characterization of most glycosyltransferases, as well as data about their localization and spatial and temporal regulation are still missing, we can only speculate about the function of the UGTs controlled by PFG factors. The two glycosyltransferases UGT91A1 and UGT84A1 might be involved in the glycosylation of specific flavonols or flavonol-glycosides (see Figure 1). Similar biochemical functions were shown for UGT73C6 and UGT78D1 which transfer sugar moieties to specific flavonols or flavonol-glycosides, for UGT78D1 which catalyzes the transfer of rhamnose to the 3-OH position of quercetin and kaempferol, whereas UGT73C6 catalyzes the transfer of glucose to the 7-OH position of flavonol 3-*O*-glycosides (Jones *et al.*, 2003). Recombinant UGT84A1 has been analyzed before *in vitro* and was shown to form glucose-esters of sinapic acid and other cinnamic acids (Lim *et al.*, 2001; Messner *et al.*, 2003), indicating an involvement of this UGT in phenylpropanoid metabolism.

Regulatory principles of flavonoid biosynthesis network

It is getting increasingly clear that in the regulation of flavonoid biosynthesis it is the rule (and not the exception) that a single target gene is controlled by a fairly high number of transcription factors. In many cases, these factors are members of the same transcription factor gene family and share the same DNA-binding domain. TT2/MYB123 is known to regulate the expression of *DFR* and *BAN* (Nesi *et al.*, 2001) and potentially other steps towards proanthocyanidin biosynthesis in the seed coat, PAP1/MYB75 regulates *PAL*, *CHS* and *DFR* (Borevitz *et al.*, 2000) and other genes required for anthocyanin biosynthesis (Tohge *et al.*, 2005), while *DFR* as well as the *ANTHOCYANIDIN SYNTHASE* (*ANS/TT18*) are targets of MYB32 (Preston *et al.*, 2004).

This network of transcriptional control is thought to be integrated at the level of the target gene by addressing similar or (at least when a single target gene is considered) identical *cis*-acting elements. In the case of R2R3-MYB transcription factors this *cis*-acting element is the MYB recognition element (MRE) (Feldbruegge *et al.*, 1997; Hartmann *et al.*, 2005) that was described previously as Box-I (Hartmann *et al.*, 1998; Kaiser and Batschauer, 1995; Schulze-Lefert *et al.*, 1989), and that is also related to the P box (Grotewold *et al.*, 1994; Lois *et al.*, 1989). The MRE

consensus sequence 5′-AcCTACCa-3′ is conserved among the promoters of the coactivated *A. thaliana FBG*s *CHS*, *CHI*, *F3H* and *FLS1* (Hartmann *et al.*, 2005) and was also detected in the *CHS* gene promoters of a number of different plant species (Hartmann *et al.*, 1998). This *cis*-acting element is also found at least once in the −600-bp to −1-bp regions of the promoters of most of the putative SG7 factors target genes listed in Table 1 (data not shown). We hypothesize that the MRE is recognized by the R2R3-MYB DNA-binding domain present in the R2R3-MYB factors, potentially with a certain subgroup specificity. The different expression patterns of the various *R2R3-MYB* genes which vary with respect to their individual temporal, spatial and stimulus-responsive transcript accumulation patterns allow us to explain the complex co-ordination of the different gene sets required for formation of a given (phenylpropanoid) compound. This adds an important aspect to the understanding of differential gene regulation. The principle of a 'one *cis*-element – many factors' type of regulation is possibly a feature of the large transcription factor gene families found in plants. This feature may turn out to significantly complicate bioinformatic prediction of target gene/transcription factor relationships.

Obviously, the pattern and timing of gene activity of the regulatory genes determine where the transcription factors can act as such. The differential expression of several functionally identical factors seems to be a more successful evolutionary approach to the creation of complex compound accumulation patterns than an increased complexity of the activity pattern of a single factor gene. This hypothesis is supported by the view that *cis*-elements are a primary target of natural selection. Promoter evolution acts not only at the level of (enzyme-coding) target genes, but also (after gene duplication) at the level of transcription factor genes.

Clearly, the promoters of the regulatory *PFG1/MYB12*, *PFG2/MYB11* and *PFG3/MYB111* genes have acquired different responsiveness to spatial (cell-type specific) information. Now, the goal is to determine what controls the regulator. To achieve this, the application of innovative technology like GFP-based fluorescence-activated cell sorting of different cell types combined with gene chip analyses, that has been shown to work for roots (Birnbaum *et al.*, 2003), should be helpful.

Experimental procedures

Standard molecular biology methods

Standard molecular biology techniques were carried out essentially as described by Sambrook *et al.* (1989). All plasmid constructions were verified by DNA sequencing. The DNA sequencing was performed using BigDye terminator chemistry on ABI 377 and 3730 sequencers (Applied Biosystems, http://www.appliedbiosystems.com/). Oligonucleotides were purchased from Metabion (http://www.metabion.com/), or Invitrogen (http://www.invitrogen.com/).

Plant material

All mutant seed stocks were in the *A. thaliana* accession Columbia-0 genetic background. Mutant alleles were identified from the SALK (Alonso *et al.*, 2003) and GABI-Kat (Rosso *et al.*, 2003) populations. Seed stocks were obtained from Nottingham Arabidopsis Stock Centre (NASC) and GABI-Kat, respectively. The *myb11* mutant carries a T-DNA insertion in *At3g62610/MYB11/PFG2* (SALK077068, NASC ID N577068), the *myb111* mutant carries a T-DNA insertion in *At5g49330/MYB111/PFG3* (GK291D01) and the *tt7*-GK349D05 mutant contains an insertion in *At5g07990/F3′H* (GK349D05; Rosso *et al.*, 2003). The *myb12*-1f and *tt4*-2YY6 mutants were described before (Mehrtens *et al.*, 2005; Saslowsky *et al.*, 2000). Sequences of characterized alleles were submitted to GenBank (DQ178603 and DQ178604 for the *myb111*-GK291D01 allele, DQ178605 and DQ178606 for the *myb11*-SALK077068 allele and DQ224277 for the *myb12*-1f allele). Homozygous double and triple mutants were produced by crossings and the progenies were analyzed using PCR markers and cleaved amplified polymorphic sequence (CAPS) markers that distinguish between mutant and wild-type alleles (see Supplementary Material).

Growth conditions

Surface-sterilized *A. thaliana* seeds were sown on 0.5× MS/1.5% sucrose/0.8% agar plates, kept for 2 days at 4°C in the dark, and then transferred to a phytochamber with 16 h of light illumination per day at 22°C. Plates were set up in vertical orientation and at the fifth day after germination (6 days after transfer into the light) seedlings were harvested.

Transfection experiments

Protoplast isolation and transfection experiments for the detection of transient expression were performed as described by Mehrtens *et al.* (2005). The flavonoid biosynthesis enzymes reporter constructs and the MYB12 effector construct have been described previously (Mehrtens *et al.*, 2005). See Supplementary Material for details of the creation of new reporter and effector constructs. In the co-transfection experiments, a total of 25 μg of pre-mixed plasmid DNA was transfected, consisting of 10 μg of reporter plasmid, 1 μg of effector plasmid and 5 μg of the luciferase (LUC) standardization plasmid. Protoplasts were incubated for 20 h at 26°C in the dark before LUC and GUS enzyme activities were measured. Specific GUS activity is given in pmol MU per mg protein per min. Standardized specific GUS activity (GUS′) was calculated by multiplication of the specific GUS activity value with a correction factor derived from the ratio of the specific LUC activity in the given sample to the mean specific LUC activity (describing the transformation efficiency) of a set of six complete experiments. The error bars indicate the standard deviation of the six GUS′ values for the respective construct.

Creation of promoter:GUS transgenic plants and GUS staining

See Supplementary Material.

Ribonucleic acid isolation

Ribonucleic acid from seedlings or parts of seedlings were isolated using the RNeasy® Plant Mini Kit (no. 74904, Qiagen, http://www.qiagen.com/) following the manufacturer's instructions.

Reverse transcriptase-PCR

Complementary DNA was synthesized from 3 μg total RNA in 20 μl volume using an oligo dT primer and SuperscriptII RT (Invitrogen) at 42°C in 1 h. One microliter of resulting cDNA was used as template in the following PCR: 25 μl volume containing 20 mM 2-amino-2-(hydroxymethyl)1,3-propanediol (TRIS)-HCl (pH 8.4), 50 mM KCl, 1.5 mM MgCl$_2$, 0.2 mM each dNTP, 0.2 μM each primer and 1.5 U *Taq* DNA polymerase (Invitrogen) using the cycling protocol: 3 min, 95°C – 33 cycles of 20 sec, 95°C; 20 sec, 57°C and 80 sec, 72°C – 2 min, 72°C. Nine microliters of the amplification products were analyzed by electrophoresis and visualized by ethidium bromide on a 1% agarose gel. The following primers were used: RS469 (5′-TCCGCTCTTTCT-TTCCAAGCTCAT-3′) and RS470 (5′-TCCAGCACAATACCGGTTGT-ACG-3′) giving a product of about 500 bp for detection of *ACT2* transcripts, RS601 (5′-CCCAAAAATGCCGGGCTAAAGAGATG-3′) and RS819 (5′-GCCAAAATCGTATTTACACATGAA-3′) for *MYB11* (1086-bp amplicon) and RS820 (5′-ATATTCAGACCAATGGTGAAGGTT-3′) and RS821 (5′-CCCATAGATCATCACTTTGACAAG-3′) for detection of *MYB111* cDNA giving a PCR product of 912 bp.

Quantitative real-time RT-PCR (qPCR)

Complementary DNA was synthesized from 2 μg total RNA after DNaseI treatment as described by Mehrtens *et al.* (2005). Quantitative PCRs analyzing the transcript level of *MYB11*, *MYB12* and *MYB111*, as well as for SG7 MYB target gene confirmation were performed using the Platinum SYBR Green qPCR SuperMix UDG Kit (Invitrogen) following the manufacturer's instructions on a Rotor-Gene 3000 DNA detection system (Corbett Research, http://www.corbettlifescience.com/). Transcript levels were normalized to 18S rRNA transcript levels. The primers were as follows: 18S rRNA, forward primer FM137 (5′-TCTGTGATGCCCTTAGATGTTCTG-3′), reverse primer FM138 (5′-GGCAAGGTGTGAACTCGTTGA-3′); *MYB11*, forward primer RS601 (5′-CCCAAAAATGCCGGGCTAAAGA-GATG-3′), reverse primer RS710 (5′-CTTCTTCGGGAGTTATGTTT-3′); *MYB12*, forward primer RS658 (5′-CACTTTGGGAAACAGGTGGT-CACT-3′), reverse primer RS709 (5′-GTTGTGGAGTTTACGGCTGA-3′); *MYB111*, forward primer RS711 (5′-AAAGAGGAAATATTACTT-CCGACGAA-3′), reverse primer RS712 (5′-TTGTCT-GTTCTTCCT-GGTAGATGTG-3′); target gene *At2g22590*, forward primer RS675 (5′-GACGAGACAGAAGGTTTCTTTAC-3′), reverse primer RS676 (5′-CCACATAACGATCTTGTCTATCC-3′); target gene *At4g15480*, forward primer RS679 (5′-GTAAAGGGATGATTGTGGATTG-3′), reverse primer RS680 (5′-CAAAGATTCCATTGTCGAGTTC-3′); target gene *At5g62210*, forward primer RS685 (5′-GACG-ATAACCAGGTG-GTCGCAC-3′), reverse primer RS686 (5′-CGTCGGTACCGGAACGG-TAGATGT-3′). Average results of two biological replicates, each with triple values, are given.

Transcriptome analysis using ATH1 gene chips

Preparation of cDNA from total RNA and hybridization to ATH1 DNA arrays (Affymetrix) were performed by the Integrated Functional Genomic (IFG) service unit of the Interdisciplinary Center for Clinical Research (IZKF) in Münster, Germany. The resulting cabinet-file (.cab) was processed using the GeneChip-Operating System (GCOS; Affymetrix). Calculations and analysis of transcriptome data were performed using MS Excel (Microsoft, http://www.microsoft.com/). Fold change was calculated as the ratio of signal intensity in the mutant to that in the wild-type plant. To reduce the number of false positives, we selected genes with 'present' absolute values out of the baseline data (arbitrarily set to $P \geq 20$). The microarray data and Minimum Information About a Microarray Experiment (MIAME)

documentation has been submitted to ArrayExpress (http://www.ebi.ac.uk/arrayexpress/), a public repository for microarray data. It could be found under accession number E-ATMX-5.

Methanolic extracts for HPLC and HPTLC analyses

Methanolic extracts from 5-dag seedlings were produced from 20–150 mg plant material in 2 ml reaction tubes by addition of 0.4 ml 80% methanol and about 10–15 zirconia beads of 1 mm diameter (Roth, http://www.carlroth.com/). Samples were homogenized at maximum speed in a Ribolyser (Qbiogene, http://www.qbiogene.com) at a setting of 6.5 msec, twice for 45 sec. Homogenized samples were incubated for 15 min at 70°C and centrifuged for 10 min at 15 000 g in a standard table centrifuge. Supernatants were vacuum-dried in a SpeedVac at 60°C. The dried pellets were dissolved in 1 μl of 80% methanol mg^{-1} starting material for HPTLC analysis and in 80% methanol containing 5 μg ml^{-1} luteolin-7-glycoside (Roth) for HPLC analysis. The digitoflavone luteolin-7-glycoside was used as an internal standard for the relative quantification of compounds.

HPLC-PDA-ESI/MS analyses

A HPLC-PDA-ESI/MS system composed of Finnigan Spectra System P4000 HPLC, UV6000 photodiode array, Autosampler AS3000 and Finnigan LCQ DECA mass spectrometer (Thermo Scientific, www.thermo.com) with a custom spray head having a spray angle of 30º was used to analyze 20 μl of the methanolic extracts. High-performance liquid chromatography was carried out on a LiChroCART C18, 4 μm, 2 ×125 mm column (Merck, http://www.merck.com/) at a flow rate of 0.2 ml min^{-1}. Solvent A was aceto-nitrile with 0.1% formic acid, and solvent B was 0.1% formic acid in water (J.T. Baker, http://www.mallbaker.com/). The elution gradient program was a linear gradient from solvent A to solvent B. The gradient program was started with 5% A (5 min), linearly increased to 25% A (30 min) and ended with 100% A (35 min). A PDA was used for detection of UV-visible absorption in the range of 200–700 nm. Nitrogen was used as the sheath gas (6 bar at a flow rate of 0.8 l min^{-1}) for the positive-ion ESI/MS which was performed at a capillary temperature and voltage of 320°C and 5.0 kV, respectively. The tube lens offset was set at 10.0 V. Full scan mass spectra were acquired from 80–2000 *m/z* at 2 scans sec^{-1}. Stepwise fragmentation analysis was carried out with different activation energies depending on the compound class.

Gas chromatography-MS analysis

The HPTLC-purified flavonol glycosides and 100 nM solutions of pure reference substances were aliquotted into 1 ml tight reacti-vials (Supelco, www.sigmaaldrich.com/Brands/Supelco_Home.html). Methanolic HCl (0.5 ml at 1.25 M concentration) was added and the samples were incubated at 80°C for 6 h. Subsequently, the samples were dried under a nitrogen stream and 50 μl of both pyridine and N-methyl-N-(trimethylsilyl) trifluoroacetamide (Macherey-Nagel, https://www.mn-net.com/) were added. The samples were stirred at 37°C for 30 min. After hydrolysis and deri-vatization, the samples were analyzed on a Trace GC/PolarisQ bench-top GC/MS system equipped with an AS 2000 autosampler (Finnigan Corp.). The GC separation was performed on a 30 m Equity5 column with 0.5 μm film thickness (Supelco). The tem-perature of the injection port was adjusted to 200°C and to 250°C for the transfer line. Helium was used as carrier gas at a flow rate of 1 ml min^{-1}. Samples of 1 μl were injected in a splitless mode. The

initial column temperature was 80°C. This temperature was held for 3 min and was gradually increased at a rate of 5°C min^{-1} to a final temperature of 325°C. To equilibrate the system for the next sample injection, the temperature was lowered to 80°C again and held constant for additional 5 min. Mass spectra were recorded with a scanning range of 50–650 *m/z* at 2 scans sec^{-1}.

High-performance thin layer chromatography with subse-quent DPBA staining

High-performance thin layer chromatography and followed by DPBA staining was performed according to Wagner and Bladt (1995). Two microliters of methanolic extracts was spotted on 10 cm × 10 cm silica-60 HPTLC-plates (Merck) used as the station-ary phase. Adsorption chromatography was carried out using a system of ethyl acetate, formic acid, acetic acid and water (100:26:12:12) as the mobile phase in a closed glass tank. Separated phenylpropanoid compounds were stained by spraying a 1% DPBA (w/v) (also known as Naturstoffreagenz A; Roth 9920-1) solution in methanol, followed by spraying 5% methanolic polyethylene glycol (PEG) 4000 (w/v) solution. The stained chromatograms were examined under UV light (312 nm) and photographed.

Flavonoid staining of whole seedlings

For the visualization of flavonoids a method from Sheahan and Rechnitz (1992) was adapted. *Arabidopsis thaliana* seedlings were grown after germination for 5 days with 16 h light per day on filter paper soaked with 3 p.p.m. of the bleaching reagent norflurazon (Supelco; PS-1044) that blocks the synthesis of carotenoids. The bleached seedlings were stained to saturation for at least 1.5 h in a freshly prepared solution of 0.25% (w/v) DPBA, 0.00375% (v/v) Triton X-100. Fluorescence was visualized on a Leica DM5500 B epifluo-rescence microscope (http://www.leica-microsystems.com/) using Leica Filtercube A with an excitation wavelength of 340–380 nm and a 425-nm long-pass splitter. Pictures were taken using the Diskus digital imaging software (version 4.50.1638) with the same imaging setting parameters for each picture series. Pictures were assembled using Adobe Photoshop (Adobe Systems Inc., http://www.adobe.com/) software without changing the color parameters.

Supplementary Material

The following supplementary material is available for this article online:
Experimental procedures. Creation of double and triple *myb* mutant(s), Genotyping of mutants, Transfection experiments, Cre-ation of promoter:GUS transgenic plants and GUS staining.
This material is available as part of the online article from http://www.blackwell-synergy.com

References

Albert, S., Delseny, M. and Devic, M. (1997) *BANYULS*, a novel negative regulator of flavonoid biosynthesis in the Arabidopsis seed coat. *Plant J.* **11**, 289–299.

Alonso, J.M., Stepanova, A.N., Leisse, T.J. *et al.* (2003) Genome-wide insertional mutagenesis of *Arabidopsis thaliana*. *Science*, **301**, 653–657.

Birnbaum, K., Shasha, D.E., Wang, J.Y., Jung, J.W., Lambert, G.M., Galbraith, D.W. and Benfey, P.N. (2003) A gene expression map of the Arabidopsis root. *Science*, **302**, 1956–1960.

Böhm, H., Boeing, H., Hempel, J., Raab, B. and Kroke, A. (1998) Flavonols, flavone and anthocyanins as natural antioxidants of food and their possible role in the prevention of chronic diseases. *Zeitschrift für Ernährungswissenschaften*, **37**, 147–163.

Borevitz, J.O., Xia, Y.J., Blount, J., Dixon, R.A. and Lamb, C. (2000) Activation tagging identifies a conserved MYB regulator of phenylpropanoid biosynthesis. *Plant Cell*, **12**, 2383–2393.

Bowles, D. (2002) A multigene family of glycosyltransferases in a model plant, *Arabidopsis thaliana*. *Biochem. Soc. Trans.* **30**, 301–306.

Brown, D.E., Rashotte, A.M., Murphy, A.S., Normanly, J., Tague, B.W., Peer, W.A., Taiz, L. and Muday, G.K. (2001) Flavonoids act as negative regulators of auxin transport *in vivo* in Arabidopsis. *Plant Physiol.* **126**, 524–535.

Buer, C.S. and Muday, G.K. (2004) The *transparent testa4* mutation prevents flavonoid synthesis and alters auxin transport and the response of Arabidopsis roots to gravity and light. *Plant Cell*, **16**, 1191–1205.

Buer, C.S., Sukumar, P. and Muday, G.K. (2006) Ethylene modulates flavonoid accumulation and gravitropic responses in roots of Arabidopsis. *Plant Physiol.* **140**, 1384–1396.

Burbulis, I.E., Iacobucci, M. and Shirley, B.W. (1996) A null mutation in the first enzyme of flavonoid biosynthesis does not affect male fertility in Arabidopsis. *Plant Cell*, **8**, 1013–1025.

Debeaujon, I., Peeters, A.J.M., Léon-Kloosterziel, K.M. and Koornneef, M. (2001) The *TRANSPARENT TESTA12* gene of Arabidopsis encodes a multidrug secondary transporter-like protein required for flavonoid sequestration in vacuoles of the seed coat endothelium. *Plant Cell*, **13**, 853–872.

Feldbruegge, M., Sprenger, M., Hahlbrock, K. and Weisshaar, B. (1997) *Pc*MYB1, a novel plant protein containing a DNA-binding domain with one MYB repeat, interacts *in vivo* with a light-regulatory promoter unit. *Plant J.* **11**, 1079–1093.

Grotewold, E., Drummond, B.J., Bowen, B. and Peterson, T. (1994) The *myb*-homologous P gene controls phlobaphene pigmentation in maize floral organs by directly activating a flavonoid biosynthetic gene subset. *Cell*, **76**, 543–553.

Harborne, J.B. and Williams, C.A. (2000) Advances in flavonoid research since 1992. *Phytochemistry*, **55**, 481–504.

Hartmann, U., Valentine, W.J., Christie, J.M., Hays, J., Jenkins, G.I. and Weisshaar, B. (1998) Identification of UV/blue light-response elements in the *Arabidopsis thaliana* chalcone synthase promoter using a homologous protoplast transient expression system. *Plant Mol. Biol.* **36**, 741–754.

Hartmann, U., Sagasser, M., Mehrtens, F., Stracke, R. and Weisshaar, B. (2005) Differential combinatorial interactions of cis-acting elements recognized by R2R3-MYB, BZIP, and BHLH factors control light-responsive and tissue-specific activation of phenylpropanoid biosynthesis genes. *Plant Mol. Biol.* **57**, 155–171.

Jacobs, M. and Rubery, P.H. (1988) Naturally occuring auxin transport regulators. *Science*, **241**, 346–349.

Jin, H., Cominelli, E., Bailey, P., Parr, A., Mehrtens, F., Jones, J., Tonelli, C., Weisshaar, B. and Martin, C. (2000) Transcriptional repression by AtMYB4 controls production of UV-protecting sunscreens in Arabidopsis. *EMBO J.* **19**, 6150–6161.

Jones, P., Messner, B., Nakajima, J., Schaffner, A.R. and Saito, K. (2003) UGT73C6 and UGT78D1, glycosyltransferases involved in flavonol glycoside biosynthesis in *Arabidopsis thaliana*. *J. Biol. Chem.* **278**, 43910–43918.

Jorgensen, K., Rasmussen, A.V., Morant, M., Nielsen, A.H., Bjarnholt, N., Zagrobelny, M., Bak, S. and Moller, B.L. (2005) Metabolon formation and metabolic channeling in the biosynthesis of plant natural products. *Curr. Opin. Plant Biol.* **8**, 280–291.

Kaiser, T. and Batschauer, A. (1995) *Cis*-acting elements of the CHS1 gene from white mustard controlling promoter activity and spatial patterns of expression. *Plant Mol. Biol.* **28**, 231–243.

Kirik, V., Schnittger, A., Radchuk, V., Adler, K., Hülskamp, M. and Baumlein, H. (2001) Ectopic expression of the Arabidopsis AtMYB23 gene induces differentiation of trichome cells. *Dev. Biol.* **235**, 366–377.

Koes, R., Verweij, W. and Quattrocchio, F. (2005) Flavonoids: a colorful model for the regulation and evolution of biochemical pathways. *Trends Plant Sci.* **10**, 236–242.

Kranz, H.D., Denekamp, M., Greco, R. *et al.* (1998) Towards functional characterisation of the members of the *R2R3-MYB* gene family from *Arabidopsis thaliana*. *Plant J.* **16**, 263–276.

Lazar, G. and Goodman, H.M. (2006) MAX1, a regulator of the flavonoid pathway, controls vegetative axillary bud outgrowth in Arabidopsis. *Proc. Natl Acad. Sci. USA*, **103**, 472–476.

Lee, M.M. and Schiefelbein, J. (2001) Developmentally distinct MYB genes encode functionally equivalent proteins in Arabidopsis. *Development*, **128**, 1539–1546.

Lepiniec, L., Debeaujon, I., Routaboul, J.M., Baudry, A., Pourcel, L., Nesi, N. and Caboche, M. (2006) Genetics and biochemistry of seed flavonoids. *Annu. Rev. Plant Biol.* **57**, 405–430.

Lim, E.K., Li, Y., Parr, A., Jackson, R., Ashford, D.A. and Bowles, D.J. (2001) Identification of glucosyltransferase genes involved in sinapate metabolism and lignin synthesis in Arabidopsis. *J. Biol. Chem.* **276**, 4344–4349.

Lingens, F. and Keller, E. (1983) Biosynthesis of phenylalanine and tyrosine: arogenic acid, a new intermediate product. *Naturwissenschaften*, **70**, 115–118.

Lois, R., Dietrich, A., Hahlbrock, K. and Schulz, W. (1989) A phenylalanine ammonia-lyase gene from parsley: Structure, regulation and identification of elicitor and light responsive *cis*-acting elements. *EMBO J.* **8**, 1641–1648.

Mehrtens, F., Kranz, H., Bednarek, P. and Weisshaar, B. (2005) The Arabidopsis transcription factor MYB12 is a flavonol-specific regulator of phenylpropanoid biosynthesis. *Plant Physiol.* **138**, 1083–1096.

Messner, B., Thulke, O. and Schaeffner, A.R. (2003) Arabidopsis glucosyltransferases with activities toward both endogenous and xenobiotic substrates. *Planta*, **217**, 138–146.

Mol, J., Grotewold, E. and Koes, R. (1998) How genes paint flowers and seeds. *Trends Plant Sci.* **3**, 212–217.

Muller, D., Schmitz, G. and Theres, K. (2006) *Blind* homologous R2R3 Myb genes control the pattern of lateral meristem initiation in Arabidopsis. *Plant Cell*, **18**, 586–597.

Murphy, A., Peer, W.A. and Taiz, L. (2000) Regulation of auxin transport by aminopeptidases and endogenous flavonoids. *Planta*, **211**, 315–324.

Nesi, N., Debeaujon, I., Jond, C., Pelletier, G., Caboche, M. and Lepiniec, L. (2000) The *TT8* gene encodes a basic helix-loop-helix domain protein required for expression of *DFR* and *BAN* genes in arabidopsis siliques. *Plant Cell*, **12**, 1863–1878.

Nesi, N., Jond, C., Debeaujon, I., Caboche, M. and Lepiniec, L. (2001) The Arabidopsis *TT2* gene encodes an R2R3 MYB domain protein

that acts as a key determinant for proanthocyanidin accumulation in developing seed. *Plant Cell*, **13**, 2099–2114.

Olsson, L.C., Veit, M., Weissenböck, G. and Bornman, J.F. (1998) Differential flavonoid response to enhanced UV-B radiation in *Brassica napus*. *Phytochemistry*, **49**, 1021–1028.

Ormrod, D.P., Landry, L.G. and Conklin, P.L. (1995) Shortterm UVB radiation and ozone exposure effects on aromatic secondary metabolite accumulation and shoot growth of flavonoid-deficient Arabidopsis mutants. *Physiol. Plant.* **93**, 602–610.

Peer, W.A., Brown, D.E., Tague, B.W., Muday, G.K., Taiz, L. and Murphy, A.S. (2001) Flavonoid accumulation patterns of *Transparent Testa* mutants of Arabidopsis. *Plant Physiol.* **126**, 536–548.

Pietta, P.G. (2000) Flavonoids as antioxidants. *J. Nat. Prod.* **67**, 1035–1042.

Preston, J., Wheeler, J., Heazlewood, J., Li, S.F. and Parish, R.W. (2004) AtMYB32 is required for normal pollen development in *Arabidopsis thaliana*. *Plant J.* **40**, 979–995.

Ramsay, N.A. and Glover, B.J. (2005) MYB-bHLH-WD40 protein complex and the evolution of cellular diversity. *Trends Plant Sci.* **10**, 63–70.

Ross, J.A. and Kasum, C.M. (2002) Dietary flavonoids: bioavailability, metabolic effects, and safety. *Annu. Rev. Nutr.* **22**, 19–34.

Rosso, M.G., Li, Y., Strizhov, N., Reiss, B., Dekker, K. and Weisshaar, B. (2003) An *Arabidopsis thaliana* T-DNA mutagenised population (GABI-Kat) for flanking sequence tag based reverse genetics. *Plant Mol. Biol.* **53**, 247–259.

Routaboul, J.M., Kerhoas, L., Debeaujon, I., Pourcel, L., Caboche, M., Einhorn, J. and Lepiniec, L. (2006) Flavonoid diversity and biosynthesis in seed of *Arabidopsis thaliana*. *Planta*, **224**, 96–107.

Sambrook, J., Fritsch, E.F. and Maniatis, T. (1989) *Molecular Cloning: A Laboratory Manual*, 2nd edn. New York, NY: Cold Spring Harbor Laboratory Press.

Saslowsky, D. and Winkel-Shirley, B. (2001) Localization of flavonoid enzymes in Arabidopsis roots. *Plant J.* **27**, 37–48.

Saslowsky, D.E., Dana, C.D. and Winkel-Shirley, B. (2000) An allelic series for the chalcone synthase locus in Arabidopsis. *Gene*, **255**, 127–138.

Schiefelbein, J. (2003) Cell-fate specification in the epidermis: a common patterning mechanism in the root and shoot. *Curr. Opin. Plant Biol.* **6**, 74–78.

Schmitz, G., Tillmann, E., Carriero, F., Fiore, C., Cellini, F. and Theres, K. (2002) The tomato *Blind* gene encodes a MYB transcription factor that controls the formation of lateral meristems. *Proc. Natl Acad. Sci. USA*, **99**, 1064–1069.

Schulze-Lefert, P., Becker-Andre, M., Schulz, W., Hahlbrock, K. and Dangl, J.L. (1989) Functional architecture of the light-responsive chalcone synthase promoter from parsley. *Plant Cell*, **1**, 707–714.

Sheahan, J.J. and Rechnitz, G.A. (1992) Flavonoid-specific staining of *Arabidopsis thaliana*. *Biotechniques*, **13**, 880–883.

Sheahan, J.J. and Rechnitz, G.A. (1993) Differential visualization of *Transparent Testa* mutants in *Arabidopsis thaliana*. *Anal. Chem.* **65**, 961–963.

Solovchenko, A. and Schmitz-Eiberger, M. (2003) Significance of skin flavonoids for UV-B-protection in apple fruits. *J Exp. Bot.* **54**, 1977–1984.

Stobiecki, M., Skirycz, A., Kerhoas, L., Kachlicki, P., Muth, D., Einhorn, J. and Mueller-Roeber, B. (2006) Profiling of phenolic glycosidic conjugates in leaves of *Arabidopsis thaliana* using LC/MS. *Metabolomics*, **2**, 197–219.

Stracke, R., Werber, M. and Weisshaar, B. (2001) The *R2R3-MYB* gene family in *Arabidopsis thaliana*. *Curr. Opin. Plant Biol.* **4**, 447–456.

Tohge, T., Nishiyama, Y., Hirai, M.Y. *et al.* (2005) Functional genomics by integrated analysis of metabolome and transcriptome of Arabidopsis plants over-expressing an MYB transcription factor. *Plant J.* **42**, 218–235.

Wagner, H. and Bladt, S. (1995) *Plant Drug Analysis – A Thin Layer Chromatography Atlas*, 2nd edn. Berlin: Springer.

Weisshaar, B. and Jenkins, G.I. (1998) Phenylpropanoid biosynthesis and its regulation. *Curr. Opin. Plant Biol.* **1**, 251–257.

Winkel-Shirley, B. (1999) Evidence for enzyme complexes in the phenylpropanoid and flavonoid pathways. *Physiol. Plant.* **107**, 142–149.

Winkel-Shirley, B. (2001) Flavonoid biosynthesis. A colorful model for genetics, biochemistry, cell biology, and biotechnology. *Plant Physiol.* **126**, 485–493.

Zimmermann, I.M., Heim, M.A., Weisshaar, B. and Uhrig, J.F. (2004) Comprehensive identification of *Arabidopsis thaliana* MYB transcription factors interacting with R/B-like BHLH proteins. *Plant J.* **40**, 22–34.